AMERICAN SOCIETY FOR MICROBIOLOGY | Journal of Virology

Synonymous Deoptimization of Foot-and-Mouth Disease Virus Causes Attenuation *In Vivo* while Inducing a Strong Neutralizing Antibody Response

Fayna Diaz-San Segundo,[a,b] Gisselle N. Medina,[a] Elizabeth Ramirez-Medina,[c] Lauro Velazquez-Salinas,[c] Marla Koster,[a] Marvin J. Grubman,[a] Teresa de los Santos[a]

Plum Island Animal Disease Center, ARS, USDA, Greenport, New York, USA[a]; Department of Pathobiology and Veterinary Science, University of Connecticut, Storrs, Connecticut, USA[b]; Oak Ridge Institute for Science and Education-Plum Island Animal Disease Center Research Participation Program, Oak Ridge, Tennessee, USA[c]

ABSTRACT

Codon bias deoptimization has been previously used to successfully attenuate human pathogens, including poliovirus, respiratory syncytial virus, and influenza virus. We have applied a similar technology to deoptimize the capsid-coding region (P1) of foot-and-mouth disease virus (FMDV). Despite the introduction of 489 nucleotide changes (19%), synonymous deoptimization of the P1 region rendered a viable FMDV progeny. The resulting strain was stable and reached cell culture titers similar to those obtained for wild-type (WT) virus, but at reduced specific infectivity. Studies in mice showed that 100% of animals inoculated with the FMDV A12 P1 deoptimized mutant (A12-P1 deopt) survived, even when the animals were infected at doses 100 times higher than the dose required to cause death by WT virus. All mice inoculated with the A12-P1 deopt mutant developed a strong antibody response and were protected against subsequent lethal challenge with WT virus at 21 days postinoculation. Remarkably, the vaccine safety margin was at least 1,000-fold higher for A12-P1 deopt than for WT virus. Similar patterns of attenuation were observed in swine, in which animals inoculated with A12-P1 deopt virus did not develop clinical disease until doses reached 1,000 to 10,000 times the dose required to cause severe disease in 2 days with WT A12. Consistently, high levels of antibody titers were induced, even at the lowest dose tested. These results highlight the potential use of synonymous codon pair deoptimization as a strategy to safely attenuate FMDV and further develop live attenuated vaccine candidates to control such a feared livestock disease.

IMPORTANCE

Foot-and-mouth disease (FMD) is one of the most feared viral diseases that can affect livestock. Although this disease appeared to be contained in developed nations by the end of the last century, recent outbreaks in Europe, Japan, Taiwan, South Korea, etc., have demonstrated that infection can spread rapidly, causing devastating economic and social consequences. The Global Foot-and-Mouth Disease Research Alliance (GFRA), an international organization launched in 2003, has set as part of their five main goals the development of next-generation control measures and strategies, including improved vaccines and biotherapeutics. Our work demonstrates that newly developed codon pair bias deoptimization technologies can be applied to FMD virus to obtain attenuated strains with potential for further development as novel live attenuated vaccine candidates that may rapidly control disease without reverting to virulence.

Foot-and-mouth disease (FMD) is one of the most highly contagious viral diseases of cloven-hoofed animals, and it is caused by FMD virus (FMDV), a member of the *Picornaviridae* family. The virus can infect over 70 species of livestock and wild animals, including cattle, swine, sheep, goat, and deer (1). FMD is listed by the International Organization of Animal Health (OIE) as a reportable disease, and severe trading restrictions are imposed upon notification of an outbreak (2). Disease outbreaks in previously FMD-free countries are initially controlled by culling of infected and in-contact animals, restriction of susceptible animal movement, disinfection of infected premises, and occasionally vaccination with an inactivated whole-virus antigen preparation (3). In countries where the disease is enzootic, animals are prophylactically vaccinated. While not hazardous to human health, an FMD outbreak carries severe economic costs. For instance, the recent United Kingdom outbreak of 2001 afforded economic losses that surpassed US$12 billion, seriously impacting the overall economy of the affected areas (4).

In addition to the inactivated whole-antigen vaccine formulation, a recombinant vaccine involving a replication-defective human adenovirus 5 that delivers empty FMDV capsids (Ad5-FMD) has been successfully tested in recent years; however, thus far this vaccine has been granted only a conditional license in the United States, and its production could be costly (5). Both the inactivated vaccine and the Ad5-FMD vaccine require approximately 7 days to induce protective immunity in swine and cattle, and the duration of immunity is shorter than that conferred by natural infection. As a result, vaccinated animals are susceptible to disease if

Received 25 August 2015 **Accepted** 4 November 2015

Accepted manuscript posted online 18 November 2015

Citation Diaz-San Segundo F, Medina GN, Ramirez-Medina E, Velazquez-Salinas L, Koster M, Grubman MJ, de los Santos T. 2016. Synonymous deoptimization of foot-and-Mouth disease virus causes attenuation *in vivo* while inducing a strong neutralizing antibody response. J Virol 90:1298–1310. doi:10.1128/JVI.02167-15.

Editor: S. Perlman

Address correspondence to Teresa de los Santos, teresa.delossantos@ars.usda.gov.

exposed to FMDV prior to 7 days or after approximately 6 months postvaccination (dpv).

It has been reported that rapid and long-lasting protection against viral infection is usually best achieved by vaccination with live attenuated vaccines (LAVs). Indeed, using attenuated viral vaccines, smallpox and rinderpest viruses have been eradicated (6–8), and measles has been eliminated from some parts of the world (9). So far, no attenuated vaccine has been successfully used against FMDV. We have previously developed a candidate for such a live attenuated vaccine by deleting the nonstructural viral protein L^{pro}-coding region (leaderless virus) (10). Despite the reduced pathogenicity of the leaderless virus in swine and cattle, animals inoculated with this mutant virus were not completely protected when exposed to wild-type (WT) virus, probably due to the very slow and limited replication of leaderless virus in the host (11). More recently, we have identified a conserved protein motif within the L^{pro}-coding region, the SAF-A/B, Acinus, and PIAS (SAP) domain (12), that represents a virulence factor. Substitutions of two conserved amino acid residues in this domain in FMDV A12 generated an attenuated mutant virus in cell culture and in swine. Interestingly, when the attenuated strain was tested as a vaccine candidate in swine, animals were completely protected even when challenged as early as 2 days postvaccination (13). However, since only two amino acid residues were replaced, reversion of the SAP mutant to virulence poses a considerable risk.

Codon usage bias is characteristic of all biological systems, since the frequencies of synonymous codon use for each amino acid are unequal (14). Codon usage bias in RNA viruses generally appears to be low, and differences in codon usage are most strongly correlated with the C+G genomic content (15). Despite the low codon usage bias, deoptimization has proven to be an effective genetic engineering technique to attenuate poliovirus, which, like FMDV, belongs to the *Picornaviridae* family of viruses. In parallel studies, Mueller et al. (16) and Burns et al. (17) showed that deoptimization of the P1/capsid regions of different strains of poliovirus using different codon substitution designs reduced virus replicative fitness in proportion to the number of replacement codons. Furthermore, Mueller et al. (16) showed a drastic effect on the specific infectivity of deoptimized mutant viruses when virulence was tested *in vivo* in a mouse model for poliomyelitis.

Independently of the "codon bias" concept, it has been demonstrated that, for reasons that are not understood, some synonymous codon pairs are used more or less frequently than statistically predicted, resulting in a particular "codon pair bias" in every examined species (18). Coleman et al. (19) developed an algorithm (synthetic attenuated virus engineering [SAVE]) that recodes a given amino acid sequence, but using different codon pairs, while controlling codon bias and the folding free energy of the RNA. By applying this technology to the genomes of poliovirus and influenza virus, viable viruses were synthesized and recovered. Interestingly, despite a 100% identity in the encoded protein sequence, severe attenuation was detected *in vitro* and *in vivo* (19–21). Analyses of the mechanisms involved in attenuation suggested that for these viruses, underrepresented codon pairs caused decreased rates of protein translation (19–21). This hypothesis has been recently supported by biochemical data indicating that codon usage affects the rate of translation or cotranslational protein folding (22). However, alternative mechanisms involving the induction of innate immunity as a result of changing dinucleotide frequency have been proposed by other authors (23). Furthermore, codon pair bias deoptimization of other viruses, including respiratory syncytial virus (RSV) (24), human immunodeficiency virus type 1 (25), dengue virus (26), and vesicular stomatitis virus (27), have also led to attenuated strains. All these reports indicate that codon and codon pair bias deoptimization can also be a useful tool to develop attenuated vaccine candidates against RNA viruses.

In this study, codon pair bias deoptimization was applied to "deoptimize" the P1 structural region of the virulent A12 strain of FMDV. The resulting deoptimized FMDV strain (A12-P1 deopt) was slightly attenuated in cell culture, reaching endpoint titers one log lower than those of WT virus. Interestingly, studies *in vivo* showed that FMDV A12-P1 deopt was highly attenuated in mice, and induced a protective immune response against lethal FMDV WT challenge even at a relative low dose, thus offering a broad margin between the dose needed to induce protection and the dose required to cause disease that killed the animals (vaccine safety margin of ~10,000). Furthermore, virulence studies in swine showed that the P1 deopt virus was also attenuated in the natural host, since a dose ~100-fold higher than the dose of homologous WT virus was required to cause equivalent disease. Interestingly, high levels of neutralizing antibodies (Abs) were detected in sera, suggesting that swine inoculated with the mutant virus could be protected against FMD. These results highlight the potential of codon pair bias deoptimization as a strategy to reduce the virulence of FMDV and possibly develop LAV candidates.

MATERIALS AND METHODS

Cells. Porcine kidney (PK) cell lines (LF-PK and IBRS-2) were obtained from the Foreign Animal Disease Diagnostic Laboratory (FADDL), Animal, Plant, and Health Inspection Service (APHIS), at the Plum Island Animal Disease Center (PIADC). Secondary PK cells were provided by the APHIS National Veterinary Service Laboratory, Ames, IA. BHK-21 cells (baby hamster kidney cells, strain 21, clone 13, ATCC CL10) were obtained from the American Type Culture Collection (ATCC, Manassas, VA). All cells were maintained as previously reported (12).

Viruses. Wild-type FMDV A12 (FMDV A12-WT) was generated from the full-length serotype A12 infectious clone pRMC35 (28). FMDV A12-P1 deopt was derived by modifying the codon pair bias in the 2,210-nucleotide (nt) complete P1-coding region using SAVE technology (19, 29). The deoptimized fragment and 355-nt flanking viral sequences were synthesized by GenScript (Piscataway, NJ). The synthetic sequence contained 489 nucleotide substitutions throughout the P1 coding region and PflM1 restriction sites for adequate cloning in the unchanged flanking L and 2B coding regions of the pRMC35 backbone (Fig. 1). Viruses were derived after electroporation of BHK-21 cells with *in vitro*-synthesized RNA as previously reported (28). Virus stocks were purified and concentrated by density gradient centrifugation in 10 to 50% (wt/vol) sucrose.

FMDV cell infections. Cultured cell monolayers were infected with FMDV at a multiplicity of infection (MOI) of 10. After 1 h of adsorption at 37°C, unabsorbed virus was removed by washing the cells with a solution containing 150 mM NaCl in 20 mM morpholineethanesulfonic acid (MES) (pH 6.0) before adding minimal essential medium (MEM) and proceeding with incubation at 37°C in 5% CO_2. Infected cells were frozen at 1, 3, 6, and 24 h, and virus titers were determined after thawing by plaque assay on BHK-21 cells. WT plaques were counted at 30 h postinfection (hpi), and P1 deopt plaques were counted at 48 hpi.

Western blotting. Cytoplasmic and nuclear cell fractions were prepared as described previously (30). Proteins were analyzed by Western blotting. eIF4G and VP1 were detected with rabbit polyclonal anti-eIF4G and in-house developed Abs, respectively. FMDV leader, 3D, and tubulin-α, were detected with monoclonal Ab (MAb) 5D8C7 (developed in-

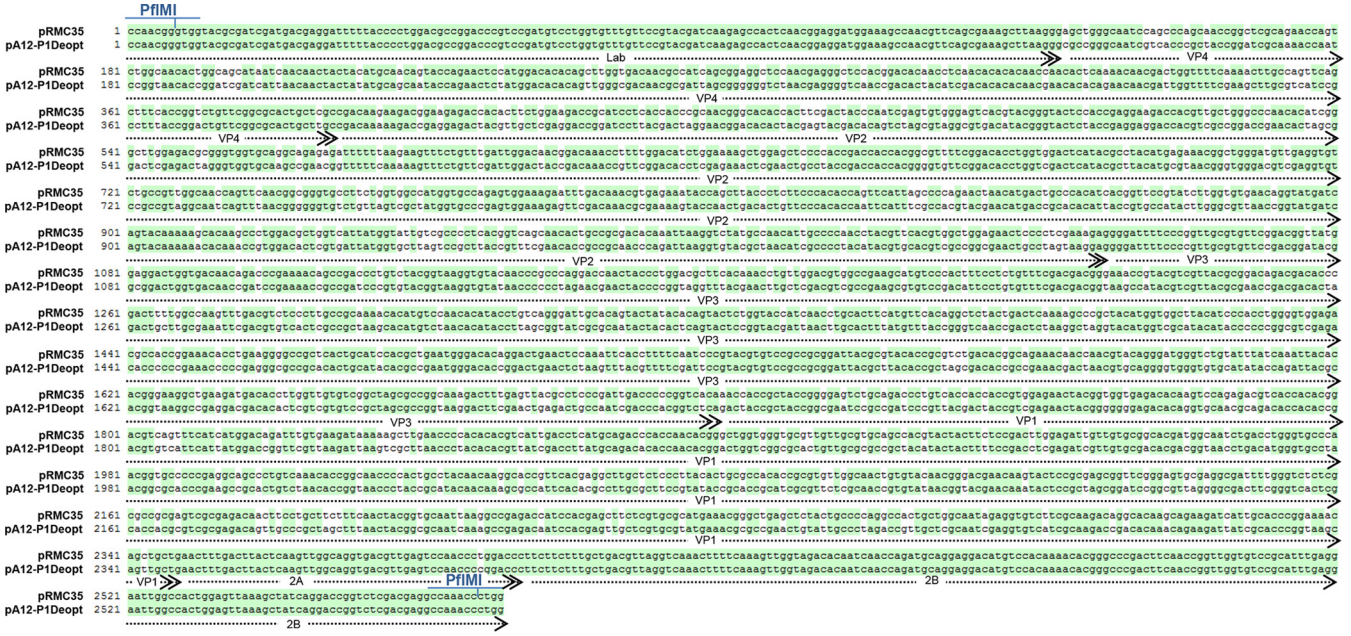

FIG 1 Global DNA alignment of the WT FMDV infectious clone (pRMC35) P1 region and the deoptimized infectious clone (pA12-P1Deopt). WT and deoptimized sequences were aligned using Clone Manager Suite V8 (Scientific & Educational Software, Morrisville, NC). The alignment includes P1 and 5′/3′ flanking regions with PflMI restriction sites (used for swapping the capsid coding region). All structural proteins within the P1 region (VP4, VP2, VP3, and VP1) are indicated, as well as nonstructural protein 2A and fragments of the 2B and L proteins.

house), F19 (305), and Ab-2 MS-581 (clone DM1A; NeoMarkers, Lab Vision), respectively.

Analysis of mRNA. A quantitative real-time reverse transcription-PCR (rRT-PCR) assay was used to evaluate the mRNA levels of porcine beta interferon (IFN-β), interferon-regulatory factor 7 (IRF7), Mx1, RANTES, tumor necrosis factor alpha (TNF-α), and interleukin-1β (IL-1β) as previously described (30).

Analysis of IFN protein. A porcine IFN-α (poIFN-α) double-capture enzyme-linked immunosorbent assay (ELISA) previously developed in our laboratory was used to quantify IFN-α protein in the supernatants of infected cells (13).

Animal experiments. Animal experiments were performed in the high-containment facilities of the Plum Island Animal Disease Center and were conducted in compliance with the Animal Welfare Act (AWA), the 2011 Guide for Care and Use of Laboratory Animals, the 2002 PHS Policy for the Humane Care and Use of Laboratory Animals, and U.S. Government Principles for Utilization and Care of Vertebrate Animals Used in Testing, Research and Training (IRAC 1985), as well as specific animal protocols reviewed and approved by the Institutional Animal Care and Use Committee (IACUC) of the Plum Island Animal Disease Center (USDA/APHIS/AC certificate number 21-F-0001).

Mouse experiments. Six- to 7-week-old female C57BL/6 mice were purchased from Jackson Laboratory (Bar Harbor, ME) and were acclimated for 1 week. In a first experiment, groups of 6 mice were anesthetized with isoflurane (Webster Veterinary, Devens, MA) and immediately infected subcutaneously (s.c.) in the left rear footpad with 10^3, 10^4, or 10^5 PFU FMDV A12-WT or with 10^5, 10^6, or 10^7 PFU of FMDV A12-P1 deopt, respectively, in a volume of 50 μl. Animals were monitored for 8 days. Viremia was determined by plaque assay on BHK-21 cells. When indicated, previously inoculated animals were challenged with 5×10^5 PFU of FMDV A12-WT s.c. in the right rear footpad. In the second mouse experiment, groups of 6 animals were s.c. inoculated in the left rear footpad with 10^1 or 10^2 PFU of FMDV A12-WT or with 10^1, 10^2, 10^3, or 10^4 PFU of FMDV A12-P1 deopt, respectively, in a volume of 50 μl. Animals were challenged at 21 days postinfection (dpi) with a lethal dose of FMDV A12-WT (5×10^5 PFU) inoculated in the right rear footpad.

Swine experiment. Twelve Yorkshire gilts (five weeks old and weighing approximately 18 to 23 kg each) were acclimated for 1 week and were subsequently divided into four groups of three animals each. Animals were inoculated intradermally (i.d.) in the heel bulb of the right hind foot with different doses of FMDV A12-P1 deopt (10^3, 10^5, 10^6, or 10^7 PFU/animal). Animals were monitored for 21 dpi. Clinical scores were determined by the number of toes presenting FMD lesions plus the presence of lesions in the snout and/or mouth. The maximum score was 17, and lesions restricted to the site of inoculation were not counted. The percentage of lymphocytes in the white cell population from whole blood collected in EDTA was measured using a Hemavet cell counter (Drew Scientific-Erba Diagnostics, Miami Lakes, FL).

Detection of virus in sera and nasal swabs. Mouse and swine sera and swine nasal swabs were assayed for the presence of virus by plaque titration on BHK-21 cells. Virus titers were expressed as $\log_{10}$ PFU per milliliter of serum or nasal secretions. The detection level of this assay is 5 PFU/ml. In addition, FMDV RNA was detected by real-time RT-PCR (rRT-PCR) as previously described (31). Forty-five amplification cycles were run, and samples were considered positive when threshold cycle (C_T) values were <40. (For details, see the footnotes to Table 2.)

Evaluation of humoral immune response. Neutralizing antibody titers were determined in mouse or swine serum samples by endpoint titration according to the method of Kärber (2). Antibody titers were expressed as the $\log_{10}$ value of the reciprocal of the dilution that neutralized the median tissue culture infectious dose ($TCID_{50}$). The presence of specific IgM and IgG Abs against FMDV in mouse sera was tested by indirect antibody sandwich ELISA as described previously (32).

Data analyses. Data handling and analysis and graphic representations were performed using Prism 5.0 (GraphPad Software, San Diego, CA) or Microsoft Excel (Microsoft, Redmond, WA). Statistical significance was determined using Student's *t* test.

RESULTS

Synonymous deoptimization of P1 results in attenuation of FMDV *in vitro*. Previous studies have shown that sequence deop-

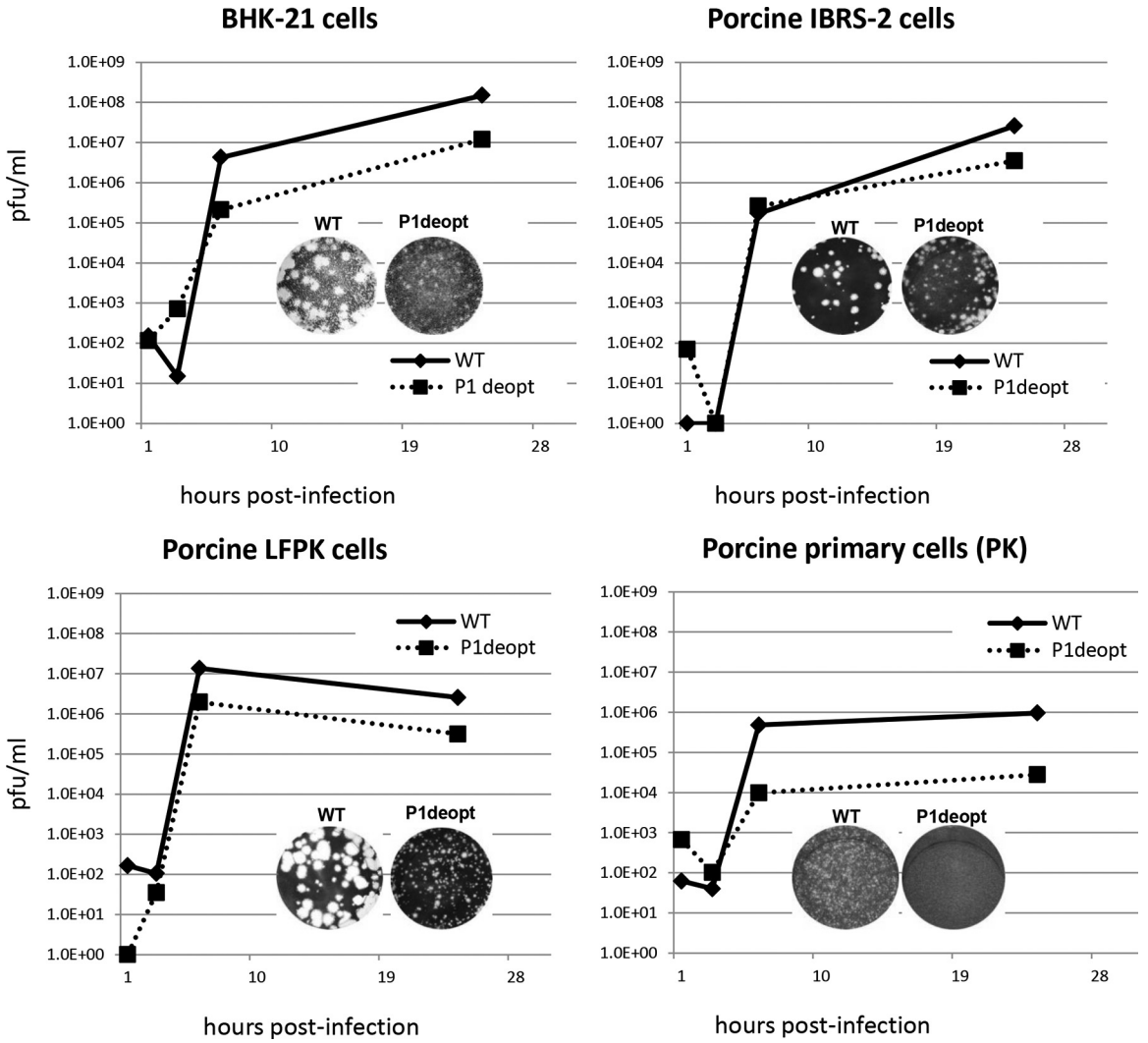

FIG 2 Kinetics of growth and plaque morphology in cell culture. Different cell lines or primary cultures were infected with A12-WT or P1-deoptimized (P1deopt) FMDV at an MOI of 10. After 1 h of incubation, unabsorbed virus was removed by washing with 150 mM NaCl–20 mM MES (pH 6.0), followed by addition of complete MEM. Infected cells were frozen at 1, 3, 6, and 24 hpi. Titers of viruses released after thawing were determined by plaque assay on BHK-21 cells.

timization is tolerated by poliovirus (19). In order to test if such a strategy would work for FMDV, which is also a member of the *Picornaviridae* family, we designed viral genomes in which the P1 region was SAVE deoptimized (19). Deoptimized sequences containing 489 nucleotide changes were synthetically obtained and subsequently replaced in the FMDV serotype A12 infectious clone (28) (Fig. 1). Electroporation of *in vitro*-synthesized A12-P1 deopt RNA rendered a viable virus that was characterized *in vitro*. Sequence analysis of A12-P1 deopt RNA showed that all nucleotide changes introduced in the P1 region were maintained after 7 passages in BHK-21 cells, and no extra changes were detected in the rest of the viral genome, at least as determined by consensus sequencing. Although before purification virus titers were slightly lower, 3×10^6 PFU/ml for P1 deopt virus compared to 5×10^7 PFU/ml for WT, high-titer viral stocks (10^8 to 10^9 PFU/ml) were obtained after concentration with polyethylene glycol (PEG) and/or purification through sucrose gradients. Viruses with P1 deoptimized displayed a small-plaque phenotype compared to the WT in all cell lines analyzed (BHK-21, IBRS-2, or LF-PK) (Fig. 2), and no plaques were detected in primary porcine kidney (PK) cells. Kinetics of growth for each particular cell line were determined by taking samples at different time points and performing plaque assays on BHK-21 cells. Although endpoint titers reached slightly lower levels in cells lacking selective innate pressure, such as porcine LF-PK and IBRS-2 or hamster BHK-21 cells, the A12-P1 deopt virus was clearly attenuated in primary porcine cell cultures, showing an almost two-log-lower virus yield at 24 h postinfection (Fig. 2). These results indicated that the growth properties of the deoptimized virus in cell culture have changed, similarly to those previously reported for attenuated FMDV strains (12, 33).

It is known that FMDV has a relatively low specific infectivity since the ratio between viral particles and infectious units (VP/PFU ratio) is relatively high and depends mostly on serotype and experimental purification procedures (34). Analysis of the virus purified by sucrose gradient centrifugation indicated that deopti-

TABLE 1 Effect of P1 deoptimization on specific infectivity

Virus and treatment[a]	Titer (PFU/ml)	VP/ml[b]	Specific infectivity (VP/PFU)
A12-WT			
PEG ppt	2.3×10^9		
SDG	8.5×10^8	4.42×10^{12}	5,200
A12-P1 deopt			
PEG ppt	4.4×10^8		
SDG	3.4×10^8	9.4×10^{12}	27,631

[a] PEG ppt, concentration by polyethylene glycol precipitation; SDG, purification by sucrose gradient centrifugation.
[b] Viral particles per milliliter, calculated by reading the optical density at 260 nm (E1% = 76).

mization of P1 reduces the specific infectivity of FMDV A12-P1 deopt by approximately 5-fold. While the VP/PFU ratio for the WT virus was about 5,000, a VP/PFU ratio of 25,000 was obtained for the P1 deopt virus concurrently grown and purified under identical experimental conditions (Table 1). These results indicated that FMDV A12-P1 deopt is attenuated *in vitro* and a higher number of particles are required to achieve the same levels of infection when no immune selective pressure is applied.

Codon pair deoptimization causes induction of the cellular innate immune response. To understand the possible mechanisms involved in attenuation caused by deoptimization, viral protein synthesis was analyzed in a time course infection at high MOI (10) in primary kidney swine cells. Western blotting analyses indicated that the levels of protein synthesis in structural (VP1) and nonstructural (leader proteinase [L^{pro}] and 3D) proteins were similar in cells infected with A12-P1 deopt or WT virus by 5 to 6 hpi. However, at earlier time points there was a slight delay in the synthesis of L^{pro} (Fig. 3A) in the cells infected with A12-P1 deopt compared to the WT virus. Consistently, a slight delay in the degradation of translation initiation factor eIF4G, which is known to be cleaved by L^{pro} (35), was detected.

It has been recently described that one of the possible mechanisms of attenuation of deoptimized viruses is the induction of an enhanced cellular innate immune response due to the increase in the number of CpG dinucleotides in the deoptimized viral mRNA

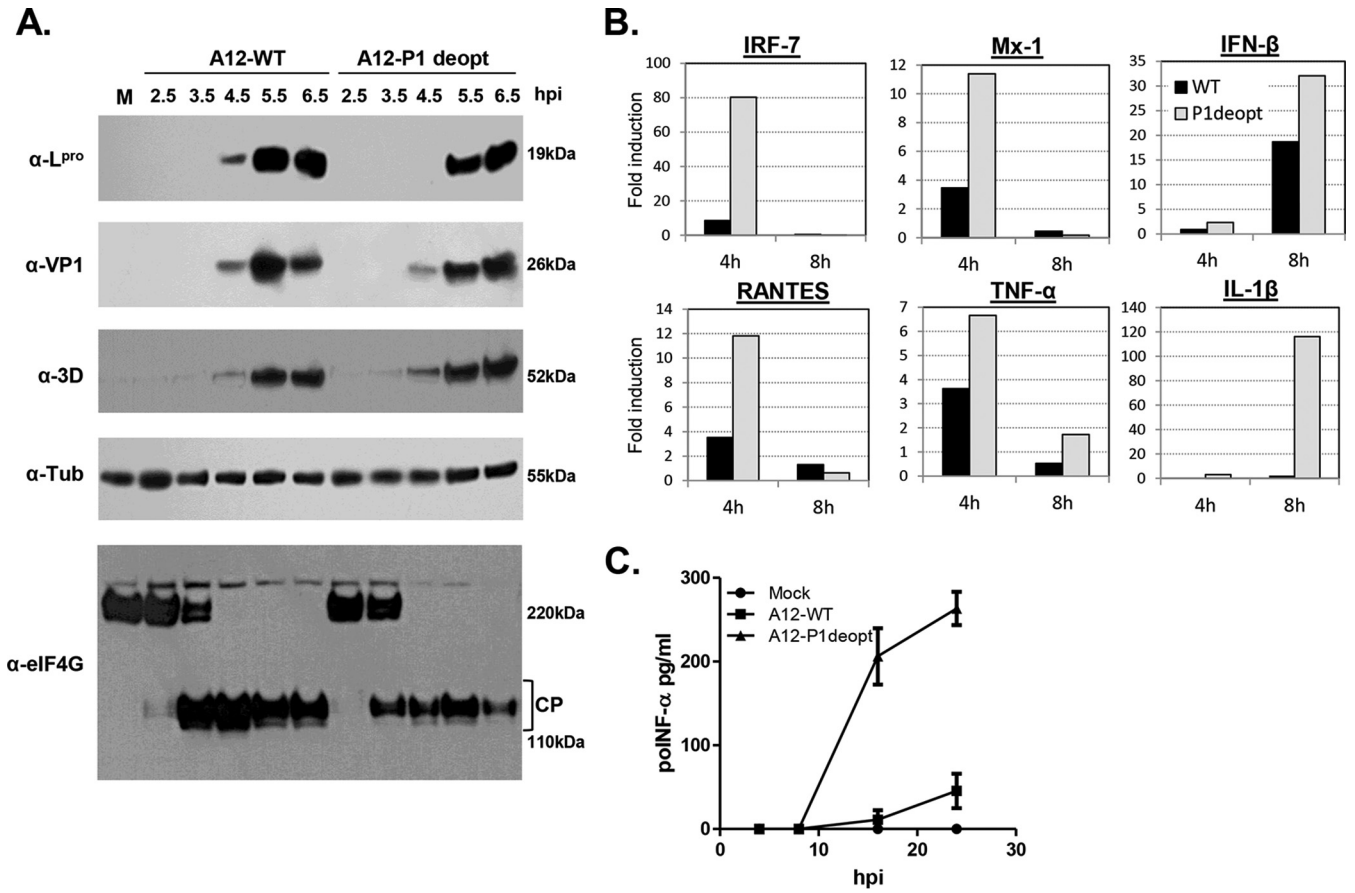

FIG 3 Analysis of viral protein synthesis, cellular protein processing, and cellular innate immune induction during infection. (A) Primary swine kidney (PK) cells were infected with A12-WT and A12-P1 deopt at an MOI of 10 for 6.5 h. At the indicated times, cytoplasmic extracts were prepared and analyzed by Western blotting using rabbit anti-eIF4G polyclonal Ab, rabbit anti-VP1 polyclonal Ab, mouse MAb 5D8C7 (anti-L^{pro}), MAb F19 (305) (anti-3D), and mouse anti-tubulin-α MAb (Ab-2 MS-581). CP, eIF4G cleavage products. (B) Expression of IFN-β, TNF-α, RANTES, Mx1, IL-1β, and IRF7 mRNAs was measured by real-time RT-PCR in PK cells infected with A12-WT and A12-P1 deopt FMDV at an MOI of 2 for the indicated times. Porcine GAPDH (glyceraldehyde-3-phosphate dehydrogenase) was used as an internal control. Results are expressed as fold increase (antilog $\Delta\Delta C_T$) of gene expression for virus-infected versus mock-infected cells (reported values display results of one out of three representative experiments with similar results). (C) Porcine IFN-α was detected by ELISA in the supernatants of PK cells infected with A12-WT and A12-P1 deopt FMDV at an MOI of 2. The values are presented as the mean ± standard deviation (SD) from three independent determinations.

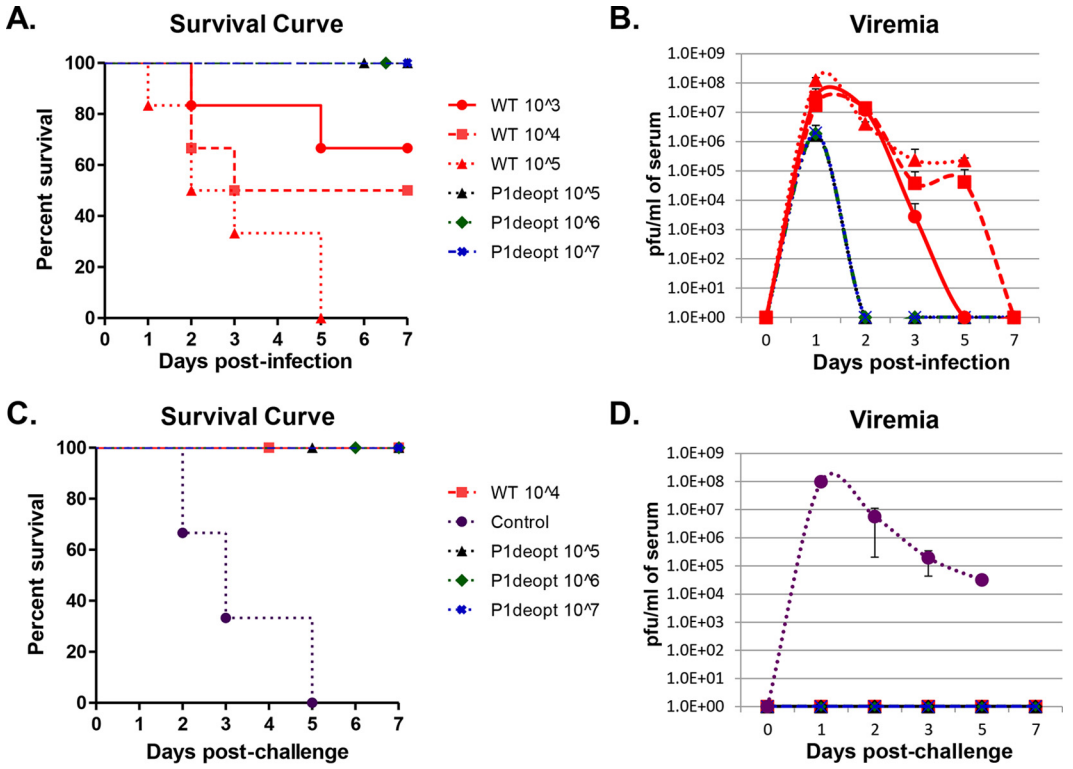

FIG 4 FMDV A12-P1 deopt is attenuated in mice. (A and B) Six- to 7-week-old female C57BL/6 mice ($n = 6$/group) were s.c. inoculated in the footpad with the indicated doses of A12-WT (WT) or A12-P1 deopt mutant (P1deopt) FMDV. Clinical disease was followed for 7 days after inoculation, and percent survival was calculated as (number of surviving animals/number of animals per group) × 100, daily (A). Serum samples collected during 7 days after inoculation were assayed for the presence of virus by plaque assay on BHK-21 cells (B). (C and D) Mice that survived the initial inoculation were challenged with 5×10^5 PFU/animal of FMDV A12-WT s.c. in the footpad. Clinical disease was followed for 7 days after inoculation, and percent survival was calculated as described above (C). Serum samples collected during 7 days after inoculation were assayed for the presence of virus by plaque assay on BHK-21 cells (D). A control naive group was included ($n = 6$). Error bars represent the variation among individual animals within a group.

sequence (23). To study this possibility, we examined the frequency of CpG dinucleotides in the deoptimized P1 region of FMDV A12 (36). Our analyses indicated that, like for other small RNA viruses, the frequency of CpG dinucleotides in the A12-WT genome is suppressed relative to the expected frequency based on its G+C content, with an observed/expected ratio of 0.83 in the P1 coding sequence of A12-WT. However, the observed/expected CpG ratio of in the P1 deopt variant virus changed to 1.35, indicating that the overall content of CpG dinucleotides had increased after deoptimization. We also analyzed the induction of IFN-β and IFN-stimulated gene (ISG) products in primary cells infected with A12-WT or A12-P1 deopt FMDV at an MOI of 2, a relatively low value to facilitate differential detection. At this MOI, and considering the low specific infectivity of FMDV, not all the cells are expected to be infected, and therefore any IFN induced signal can be amplified by its paracrine effect on surrounding noninfected cells (37). As observed in Fig. 3B, the levels of IRF7, Mx-1, and RANTES ISG products were upregulated early upon infection with A12-P1 deopt virus compared with those in WT-infected cells, and IFN-β upregulation was higher at later time points (8 h). Also, the levels of proinflammatory cytokines were highly upregulated in cells infected with A12-P1 deopt compared to A12-WT virus, with TNF-α, increasing at relatively early times (4 h) and IL-1β at later time (8 h) postinfection. Consistent with these results, supernatants from infected cells contained significantly higher levels of accumulated poIFN-α protein by 16 to 24 hpi (Fig. 3C), indicating that the deoptimization of the genomic sequence had an effect on the cellular innate immune response induced by FMDV A12-P1 deopt infection.

Synonymous deoptimization of P1 results in attenuation of FMDV *in vivo* in mice. Salguero et al. (38) demonstrated that certain strains of adult mice, including C57BL/6 mice, are susceptible to FMDV serotype C when infected s.c. in the footpad. Infected animals developed significant viremia and die within a few days of infection. We have previously confirmed that this model is also an efficient tool for other FMDV serotypes, including A and O (39). To examine the virulence of A12-P1 deopt FMDV *in vivo*, we used the same mouse model system. Six- to 7-week-old female C57BL/6 mice were inoculated with different doses of FMDV A12-P1 deopt or FMDV A12-WT (6 mice/group) and checked for survival, viremia, and clinical signs for 8 days.

Animals inoculated with FMDV A12-WT developed clinical signs, including lethargy and rough fur, and began dying by 24 to 48 h postinoculation. As expected, all animals inoculated with 10^5 PFU of WT virus died by day 5, and this effect was dose dependent, since only 50% of mice inoculated with 10^4 PFU and 33% of mice inoculated with 10^3 PFU died by 8 dpi (Fig. 4A). None of the animals inoculated with FMDV A12-P1 deopt showed clinical signs or died even when high doses, such as 10^7 PFU/animal, were used (Fig. 4A). As previously reported, FMDV A12-WT-inocu-

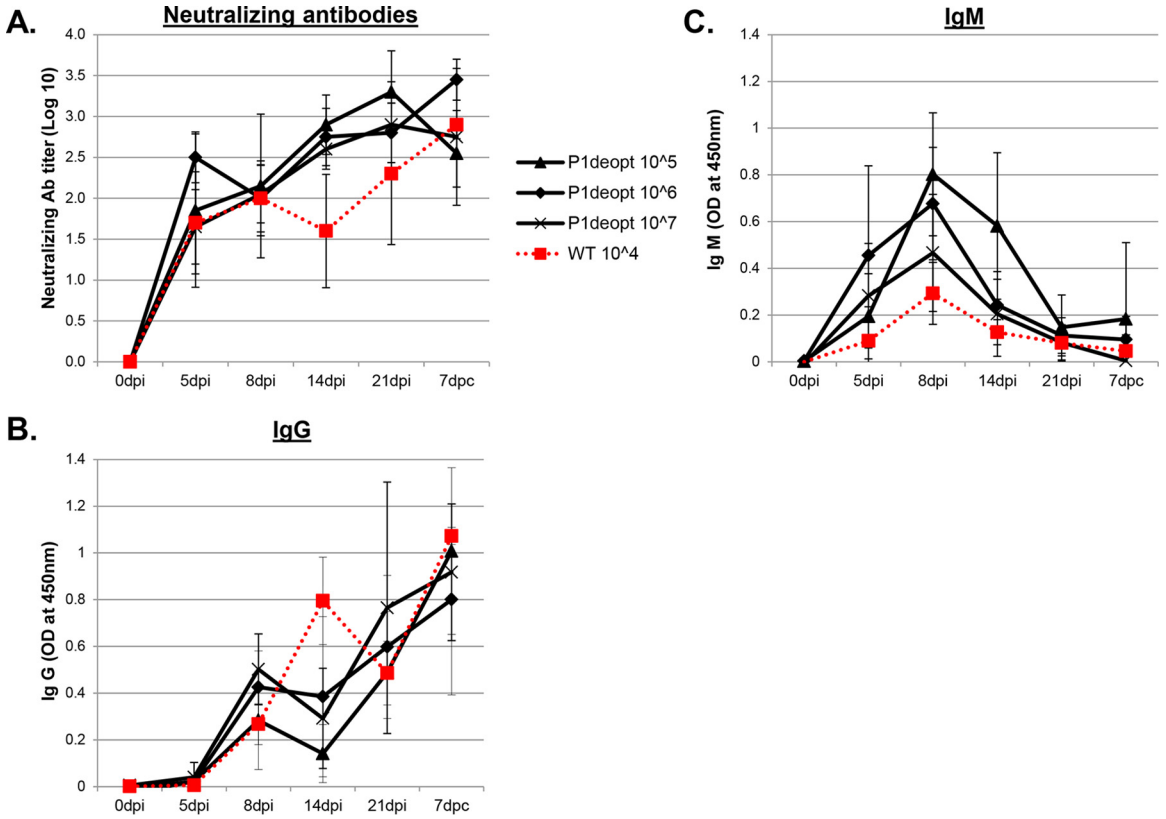

FIG 5 Humoral response induced by FMDV A12-P1 deopt in mice. (A) Neutralizing antibodies in sera of mice inoculated with FMDV A12-P1 deopt or A12-WT before (dpi) and after (dpc) challenge. Titers are expressed as the inverse dilution of serum yielding a 50% reduction of virus titer ($\log_{10}$ $TCID_{50}$/ml). Each data point represents the mean (± SD) for each group. (B and C) Systemic IgG (B) and IgM (C) antibodies in sera of mice inoculated with indicated doses of FMDV A12-P1 deopt or A12-WT before (dpi) and after (dpc) challenge. Each data point represents the mean (± SD) for each group.

lated animals showed viremia for several days after inoculation, with a peak of 10^7 to 10^8 PFU/ml at 1 dpi (Fig. 4B). In the groups inoculated with FMDV A12-P1 deopt, viremia was detected only at 1 dpi, with levels of 1.5×10^6 to 2×10^6 PFU/ml (Fig. 4B). These results indicate that FMDV A12-P1 deopt is attenuated *in vivo* in mice and does not cause death or clinical signs even at doses 10,000 times higher than WT, although virus can be detected in serum.

A12-P1 deopt FMDV induces a protective immune response in mice. In order to study whether FMDV A12-P1 deopt virus was able to induce a protective immune response, we challenged the animals originally inoculated with this virus at 21 days with 5×10^5 PFU/mouse of FMDV A12-WT, a dose 5 times higher than the dose required for this virus to cause death in all naive animals (13). We included a naive control group to ensure that the challenge dose was adequate to induce clinical disease within 24 to 72 h postchallenge and subsequently caused death. As shown in Fig. 4C, all animals in the naive control group developed disease and died by 5 days postchallenge (dpc). Viremia was detected during 5 days and peaked at 1 dpc (Fig. 4D). In contrast, all animals previously inoculated with FMDV A12-P1 deopt were protected against challenge (Fig. 4C). Furthermore, these animals did not show viremia after challenge (Fig. 4D). At the same time, animals that survived the previous inoculation with 10^4 PFU of FMDV A12-WT were also completely protected against challenge (Fig. 4C and D).

To understand the nature of protection observed in these animals, we analyzed the humoral immune response induced by FMDV A12-P1 deopt compared with the WT virus before and after challenge (Fig. 5). The levels of systemic neutralizing Abs early after inoculation induced by FMDV A12-P1 deopt were equivalent to the levels induced by WT virus, independently of the dose used, and the antibody titers were maintained in all groups at 14 and 21 days after inoculation (Fig. 5A). Interestingly, although class switching to IgG occurred at the same time and the overall IgG levels were not statistically significantly different among the groups, the levels of IgM induced by the mutant virus were higher than those elicited by WT virus (Fig. 5B and C).

These results indicated that inoculation of mice with FMDV A12-P1 deopt results in a strong protective humoral response against challenge with WT virus.

The A12-P1 deopt minimal protective dose is at least 10,000-fold lower than the infectious dose. The results described above led us to design a second mouse experiment lowering the dose of A12-P1 deopt mutant FMDV to determine the minimal dose needed to induce protection against lethal challenge with homologous WT FMDV. Six- to 7-week-old female C57BL/6 mice were vaccinated with different doses of FMDV A12-P1 deopt (10^1, 10^2, 10^3, or 10^4 PFU) or FMDV A12-WT (10^1 or 10^2 PFU) (6 mice/group). Animals were challenged at 21 days postvaccination (dpv) with FMDV A12-WT at a dose of 5×10^5 PFU/mouse in the opposite rear footpad, and disease was followed for 7 days after the

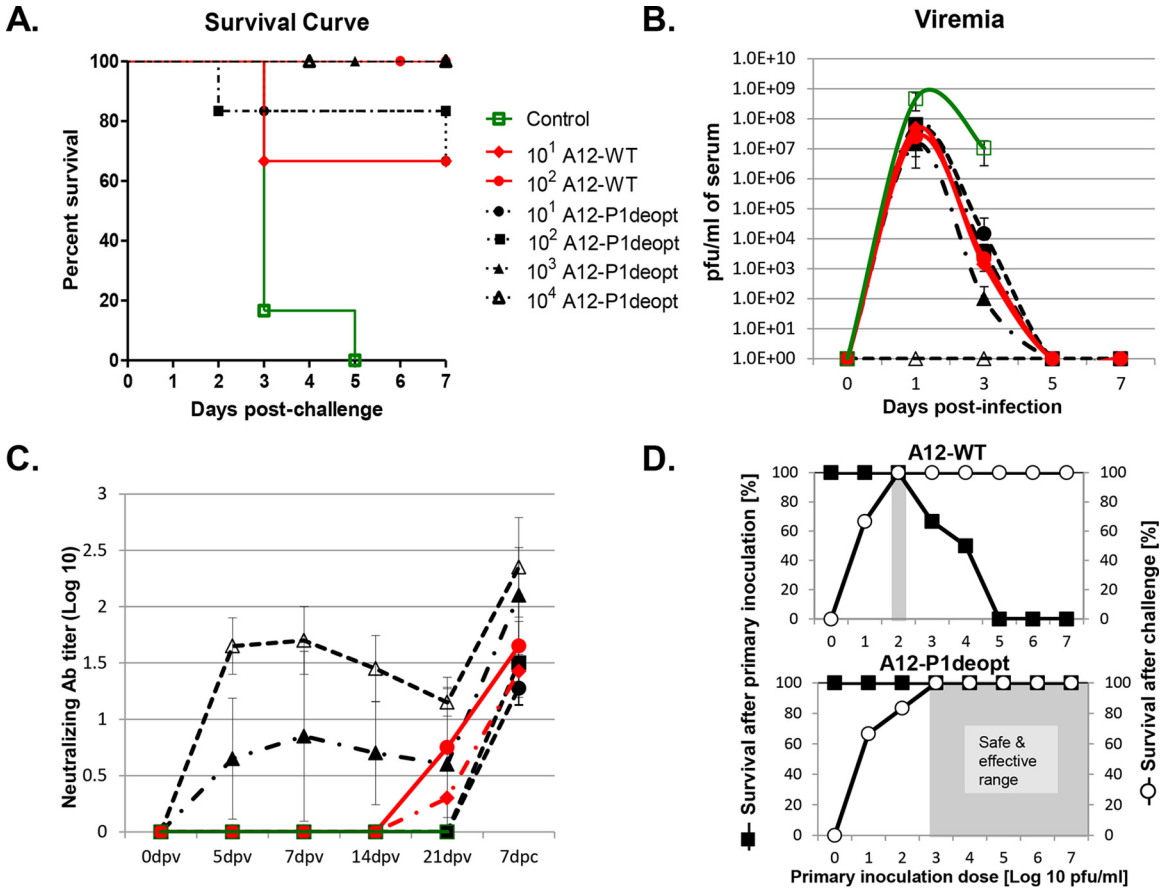

FIG 6 Minimal protective dose and safe and effective vaccine range. (A and B) Six- to 7-week-old female C57BL/6 mice ($n = 6$/group) were s.c. vaccinated with the indicated low doses of FMDV A12-WT or A12-P1 deopt mutant and challenged 21 days after vaccination (dpv) with a lethal dose of FMDV A12-WT. Clinical disease was followed for 7 days after inoculation, and percent survival was calculated as (number of surviving animals/number of animals per group) · 100 daily (A). Serum samples collected during 7 days after inoculation were assayed for the presence of virus by plaque assay on BHK-21 cells (B). (C) Neutralizing Abs in sera of mice inoculated with FMDV A12-P1 deopt or A12-WT before (dpv) and after (dpc) challenge. Titers are expressed as the inverse dilution of serum yielding a 50% reduction of virus titer ($\log_{10}$ $TCID_{50}$/ml). Each data point represents the mean (± SD) for each group. (D) Vaccine margin of safety for A12-P1 deopt or A12-WT virus. The left ordinate indicates the percentage of animals surviving the primary inoculation (black squares) with either virus at doses ranging between 10^0 and 10^7 PFU. After 21 days, the surviving, vaccinated animals were challenged with a single lethal dose of FMDV A12-WT. Survival was monitored (right ordinate; open circles) for A12-P1 deopt (top panel)- or A12-WT (bottom panel)-vaccinated mice. Gray boxes represent the margin of safety.

challenge. A control group immunized with phosphate-buffered saline (PBS) was included. As previously described, the animals in the control group developed disease and died between 3 and 5 days postchallenge and showed levels of viremia of over 10^8 PFU/ml of serum (Fig. 6A and B). Animals vaccinated with the lowest dose (10^1 PFU) of either WT or deoptimized virus showed partial protection, with 66.67% survival and levels of viremia at an average of 4.7×10^7 or 3.9×10^7 PFU/ml of serum, respectively (Fig. 6A and B). Furthermore, there was a clear dose-dependent protection, since animals vaccinated with 10^2 PFU of A12-P1 deopt virus showed 83.3% survival and survival was 100% at any higher dose. Also, levels of viremia after challenge were vaccine dose dependent, with lower levels of viremia even at the highest tested vaccination dose and with no detectable viremia in the group vaccinated with 10^4 PFU (Fig. 6B).

The presence of neutralizing Abs was detectable as early as 5 dpv for the groups vaccinated with the highest doses of A12-P1 deopt attenuated FMDV (10^3 and 10^4 PFU) (Fig. 6C). However, no neutralizing Abs were detected before challenge in animals inoculated with lower doses of A12-P1 deopt virus (10^1 to 10^2 PFU). In contrast, animals inoculated with low doses of A12-WT FMDV developed a modest induction of neutralizing Abs before the challenge (21 dpv) (Fig. 6C). As expected, there was an increase in the Ab titer after the challenge due to the boost effect of the challenge virus.

It is known that LAVs stimulate an excellent immune response that is comparable to that induced by infection with the WT pathogen (40). However, LAVs can be less safe than inactivated vaccines, since they can cause disease if inoculated at a high enough dose or in immunocompromised individuals (41). The difference between the dose needed to induce protection and the dose needed to induce disease is defined as the vaccine safety margin. Figure 6D represents the relationship between protective and lethal doses for A12-WT and for attenuated A12-P1 deopt viruses. A12-WT showed a full protective dose with 10^2 PFU. However, increasing the dose of WT virus only one log (10^3 PFU) led to a lethal infection, thus resulting in a narrow safety margin (10-fold). In contrast, although the attenuated A12-P1 deopt virus required a higher dose to induce 100% protection (10^3 PFU), it did not cause disease even when used at 10^7 PFU/animal, a dose 10,000-

TABLE 2 Experimental design and clinical performance for swine inoculated with various doses of FMDV A12-P1 deopt

Dose[a] (PFU)	Pig no.	Clinical score[b]	Viremia[c]	RT-PCR, serum[d]	Shedding virus	RT-PCR, nasal swab[e]	SN[f] at dpi:		
							7	14	21
10^3	1	0	0	N	0	N	0	2.4	2.4
	2	0	0	N	0	N	0	3	1.8
	3	0	0	N	0	N	1.2	2.1	2.4
10^5	4	0	0	N	0	N	1.8	2.4	1.8
	5	0	0	N	0	N	1.5	2.1	1.8
	6	0	0	N	0	N	0.9	4.2	2.7
10^6	7	7/1	0	WP (5–6)	0	WP (3–4)	2.1	4.8	3.9
	8	3/8	0	WP (2–4)	0	WP (3–4)	3.6	4.8	3.9
	9	4/11	$2/2.1 \times 10^3/1$	SP (1–4)	0	WP (3–4)	3.6	4.2	3.3
10^7	10	2/12	$1/8.8 \times 10^2/2$	SP (1–3)	0	WP (2–5)	3.6	3.6	3
	11	3/12	$1/4 \times 10^2/3$	SP (1–4)	0	WP (2–5)	2.7	3.9	3
	12	2/8	$1/8.5 \times 10^2/3$	SP (1–3)	0	WP (2–5)	2.4	2.7	3

[a] Dose of inoculum per animal, expressed as number of PFU in a total volume of 0.4 ml, administered by intradermal inoculation in the heel bulb.
[b] Day postchallenge for first signs of lesions/highest lesion score.
[c] First day postchallenge that viremia was detected by virus isolation/maximum amount of viremia in PFU per milliliter detected in serum samples/duration (days) of viremia.
[d] N, negative ($C_T > 40$); WP, weak positive ($30 \leq C_T < 40$); SP, strong positive ($C_T < 30$). The days at which virus was present are indicated in parentheses.
[e] N, negative ($C_T > 40$); WP, weak positive ($30 \leq C_T < 40$); SP, strong positive ($C_T < 30$). The days at which virus was present are indicated in parentheses.
[f] SN, serum neutralizing antibody titer, reported as $\log_{10}$ of the inverse of the serum dilution that neutralized 100 $TCID_{50}$ of virus in 50% of the wells at the indicated time points.

fold higher. These results clearly show that the safety margin for A12-P1 deopt is at least 1,000-fold greater than the safety margin for the WT virus.

Synonymous deoptimization of P1 results in attenuation of FMDV *in vivo* in swine. To test the virulence of FMDV A12-P1 deopt in the natural host, groups of three pigs were inoculated i.d. in the rear heel bulb with different doses of the deoptimized virus. Animals were inoculated with 10^3, 10^5, 10^6, or 10^7 PFU/animal of A12-deopt virus (Table 2), doses that we had previously shown caused clinical disease in swine inoculated with the WT virus (13).

No clinical signs were detected in animals inoculated with 10^3 or 10^5 PFU of A12-P1 deopt virus throughout the experiment (Fig. 7, bars). Similarly, no virus or viral RNA was detected in serum or nasal swabs, as measured by virus isolation and rRT-PCR (Table 2). When the dose of virus was increased to 10^6 PFU, two out of three animals (animals 8 and 9) developed clinical signs at 3 to 4 dpi with lymphopenia (Fig. 7, lines) associated with the appearance of vesicles, but disease was less severe than that observed for WT FMDV, even at doses at least 10 times lower (13). One animal (animal 7) developed clinical signs only by 7 dpi and never had lymphopenia. Consistent with the clinical data, two animals with clinical signs showed viremia by virus isolation and presence of viral RNA by rRT-PCR, and the animal that showed a late disease onset had low levels of viral RNA in serum (Table 2). All animals had detectable viral RNA in nasal swabs for 2 days. Animals inoculated with 10^7 PFU showed clinical signs starting by 2 to 3 days, with a lesion score between 8 and 13 (out of a possible maximum of 17), and had clear lymphopenia (Fig. 7); virus was detected in serum by both techniques used, and viral RNA was detected in nasal swabs for 4 days (Table 2). These results showed that there is a dose-dependent attenuation and that even at high doses (i.e., 10^7 PFU/animal) the severity of disease was reduced compared to that of the disease observed in animals inoculated with 10^5 PFU/animal of A12-WT.

FMDV A12-P1 deopt elicits a strong adaptive immune response in swine. Natural FMDV infection is cleared by the induction of a strong neutralizing antibody response that could start as early as 4 dpi, with a peak at 14 dpi. In the current experiment, we observed that despite the absence of viremia for the animals inoculated with 10^3 or 10^5 PFU of A12-P1 deopt, all the animals in these two groups developed significant levels of FMDV-specific neutralizing Abs starting at 7 dpi, with a peak at 14 dpi (Table 2). There was a clear dose response in the antibody titer at 7 dpi, and the groups administered high doses (10^6 to 10^7 PFU) overall developed higher antibody titers throughout the experiment. Nevertheless, even at the lower doses, the neutralizing antibody titers were high enough to predict protection (11).

DISCUSSION

Live attenuated vaccines have proven to be the most successful at eradicating and decreasing the incidence of viral diseases. Indeed, smallpox and rinderpest have been the only two viral diseases eradicated, after the enforcement of a series of health policy measures that included the use of LAVs (6–8). Furthermore, outbreaks of measles have been relatively limited because of the use of an effective live vaccine (9). Vaccines of this type have the advantage of closely mimicking the viral infection, thus eliciting the many responses that the host spontaneously triggers to eliminate the pathogen. In some instances, immunity elicited by the natural infection can last for life (42). Traditionally, LAVs were derived by repeated passage of virulent virus in tissue culture or in alternate hosts, resulting in the spontaneous accumulation of mutations and a decrease in virus fitness, thus generating attenuation. Despite the success of this method, evidence suggested that the attenuation could be due to just few among the many introduced mutations, highlighting the possible danger of reversion to virulence (43).

With the advancement of genetic engineering over the last 20 years, viral infectious clones were easily derived. However, manip-

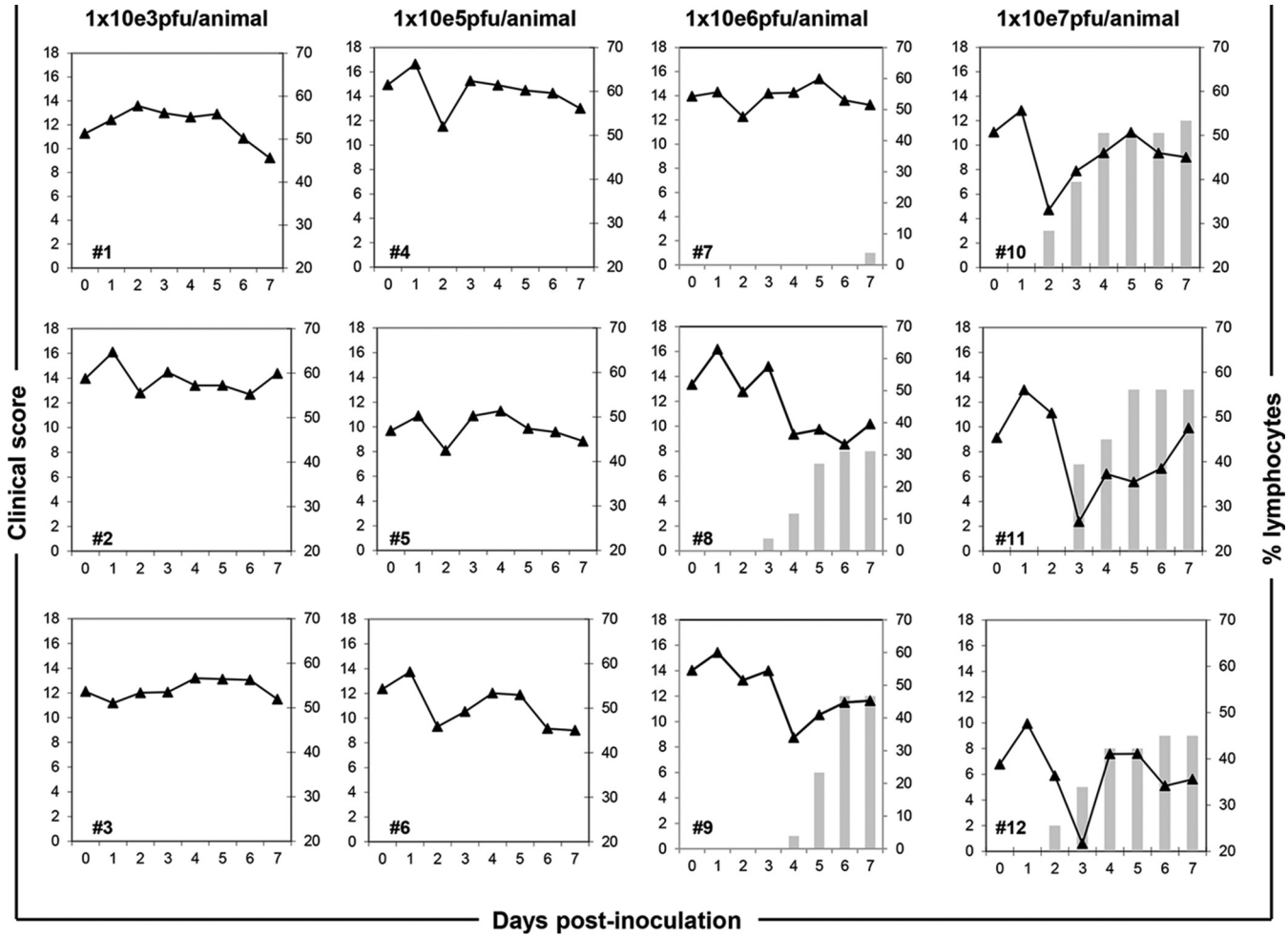

FIG 7 FMDV A12-P1 deopt is attenuated in swine. Eighteen- to 23-kg female Yorkshire swine ($n = 3$/group) were i.d. inoculated with indicated doses of the A12-P1 deopt mutant, and disease was followed for the next 7 days. The percentage of lymphocytes in blood (lines) and clinical score (bars) are represented. Clinical scores were determined by the number of toes presenting FMD lesions plus the presence of lesions in the snout and/or mouth. The maximum score was 17, and lesions restricted to the site of inoculation were not counted. Each graph represents the results observed in each individual animal.

ulating viral genomes to obtain attenuated strains can be challenging, given that small RNA viruses have evolved to simply contain the minimum genetic information required for fitness and adaptation to the host(s). Similar to the case for other picornaviruses, FMDV has a small genome, and only small deletions are tolerated without compromising viral replication. Indeed, FMDV attenuated strains containing deletions have been successfully derived. For instance, a virus lacking the leader-coding region was generated without significantly affecting replication in tissue culture (10). However, studies *in vivo* showed that the "leaderless virus" was too attenuated and induced only a limited immune response, not sufficient to protect cattle against homologous challenge (11). Interestingly, the leaderless virus behaved like WT virus when it was used like the traditional inactivated FMD vaccine (inactivated antigen in formulation with oil adjuvant), suggesting that the leaderless virus could be an alternative safer option for FMD vaccine production (11, 40, 41).

More recently, we have developed an attenuated FMDV strain with point mutations in the leader-coding region (12). Remarkably, this virus was fully attenuated in swine and induced an early protective immune response (at 2 dpv) against challenge with WT virus (13). However, given the low fidelity of viral RNA polymerases, point mutations are prone to be corrected during viral replication or new compensatory mutations may appear, posing a high risk of reversion to virulence (42).

Codon bias deoptimization is being developed as a new technology in attenuated vaccine development. Since deoptimization is due to the summation effect at each of hundreds or thousands of nucleotide mutations without changing amino acid sequences, the likelihood of reversion to virulence is expected to be reduced. Indeed, this technology has proven useful to derive attenuated strains of positive-strand RNA viruses such as poliovirus (16–18), porcine reproductive and respiratory syndrome virus (PRRSV) (29), and dengue virus (26), as well as those of negative-sense RNA viruses such as influenza virus (20), respiratory syncytial virus (24), and vesicular stomatitis virus (27).

In this study, we have investigated the feasibility of applying SAVE, a recently developed technology that modifies codon pair bias, to aphthoviruses. Our overarching goal was to derive attenuated strains of FMDV that could be further used for pathogenesis studies and potentially exploited for novel vaccine development. Based on the success of this technology with polioviruses (16, 19),

we also redesigned the viral P1-coding region in FMDV serotype A12. The P1-coding region is highly variable among the seven FMDV serotypes and codes for viral structural proteins that mostly determine antigenicity and mediate the interaction of the virus with host cell receptors. Interestingly, deoptimization of the entire P1 region was tolerated by FMDV, since a viable progeny was obtained, as opposed to the case for poliovirus, where only deoptimization of partial P1 sequences allowed for virus recovery (19). However, similar to the case for polioviruses (16) but in contrast to that for influenza virus (20), the specific infectivity for FMDV was considerably reduced, from approximately 5,000 VP/PFU for the WT to 25,000 VP/PFU for the A12-P1 deopt variant. In addition, the deoptimized virus had a small- or no-plaque phenotype, and final titers in one-step growth kinetics in primary cells were 1 to 2 logs lower than those of WT virus, indicating that the deoptimized virus was clearly attenuated *in vitro*. Although FMDV plaque morphology is heterogeneous and varies with serotype, cell line, method of detection, replicative ability, differential utilization of cellular receptors, etc. (33), similar results had been previously reported for attenuated strains of FMDV, such as leaderless and SAP mutants, particularly when the virus was grown in primary cells that maintain the immune selective pressure (12, 44). We observed only a slight delay in translation of L^{pro} and processing of eIF4G for the P1 deopt virus compared to the WT virus (Fig. 3A); however, it is important to mention that all infections were performed at similar MOIs, thereby using at least a 5-fold excess of mutant compared to WT virus, when considering its lower specific infectivity. Our results thus may mask any small but significant difference in the rate or efficiency of translation. Furthermore, it is also possible that even when the overall kinetics of viral protein synthesis was apparently not affected, the activity of individual proteins might have been compromised, thus hindering the ability of FMDV to counteract the innate response against viral infection. In fact, we and others have shown that FMDV L^{pro}, the first nonstructural protein in the FMDV open reading frame (ORF), plays a fundamental role in blocking the expression of IFN and IFN-induced genes (12, 13, 22, 44, 45).

Our analyses *in vitro* also showed that infection with the attenuated A12 -P1 deopt strain induced a strong innate cellular immune response, as several ISGs were upregulated. It is known that during viral infection, detection of foreign nucleic acids is responsible for the specific induction of transcription of IFN genes and ISGs in infected cells (46). In particular it has been shown that picornavirus RNAs are detected by the cytosolic RNA receptor MDA5 (47, 48). In fact, it has been reported that FMDV RNA is sensed through MDA5 (49). As mentioned above, in our assays, infections were performed based on equivalent PFU (infectious units). The stronger induction of ISGs for the P1 deopt in comparison to the WT virus may represent the outcome of using 5-fold-larger amounts of input viral RNA readily sensed by cellular innate receptors such as MDA5. Alternatively, the utilization of underrepresented codon pairs in the A12-P1 deopt virus may have influenced the rate of translation, as previously reported for other viruses (19–21). Even a slight reduction in the rate of L^{pro} synthesis or in its catalytic activity (Fig. 3A) could have led to slower processing of eIF4G and subsequently larger amounts of IFN and ISG products available to limit virus replication and cause attenuation. Furthermore, elegant biochemical assays have recently demonstrated that codon usage influences the rate of translation or cotranslational protein folding, potentially affecting protein function (22). These hypotheses are all well suited to explain the results obtained after deoptimizing the P1 region of FMDV A12.

It has also been hypothesized that altering the frequency of CpG and UpA dinucleotides without modifying the encoded amino acid sequence of a particular protein(s) may also play a role in viral attenuation (23). Indeed, RNA viruses have, in general, a low dinucleotide frequency (50, 51), and an increase in CpG or UpA dinucleotide content in the genomes of picornaviruses results in variants that are debilitated in growth (17, 23) or nonviable (16). Comparative analysis of the viruses used in our studies showed that the A12P1 deopt virus had an increased dinucleotide frequency, and this might be one possible reason for the observed attenuation; however, at this point, codon pair and dinucleotide biases have not been functionally distinguished, and the topic remains highly controversial (52, 53).

A12-P1 deopt virus was also attenuated *in vivo*. Using an FMD mouse model (38), the 50% lethal dose (LD_{50}) for the WT virus is 93,000 PFU However, even after inoculating a 1,000-fold-higher dose of deoptimized virus, all mice survived. Interestingly, when A12-P1 deopt-inoculated mice were further challenged with a lethal dose of homologous WT FMDV, animals were completely protected, no viremia was detected, and protection correlated with a strong neutralizing antibody response. Lowering the initial dose of inoculation (or vaccination) to 10^3 PFU still resulted in 100% protection, leaving a remarkably desirable wide safety margin of at least 10,000-fold.

Attenuation was also detected in swine, an FMDV natural host. Animals inoculated with doses of 10^3 and 10^5 PFU of A12-P1 deopt did not show any clinical sign of disease, viremia, or virus shedding, in contrast to animals inoculated with WT virus, which developed severe disease at doses of 10^5 PFU/animal or less (13). Only when A12-P1 deopt was used at doses 100-fold higher (10^7 PFU/pig) did it cause disease similar to that induced by 10^5 PFU of WT virus. The levels of neutralizing Abs induced in all A12-P1 deopt-inoculated animals, even those inoculated with the lowest dose, 10^3 PFU, were predictive of protection (11). In fact, animals inoculated with as little as 10^3 PFU of A12-P1 deopt and challenged with 10^6 PFU of homologous virus did not show clinical signs or develop detectable viremia (data not shown). Considering the data obtained in mice, inoculation of swine or other livestock species with lower virus doses, i.e., 10^2 or even 10^1 PFU/animal, might be sufficient for inducing protection, thus highlighting the potential use of these viruses as live attenuated strains for vaccine production. However, more experiments are needed to determine the actual ratio between the 50% infectious dose (ID_{50}) and the 50% protective dose (PD_{50}).

Sequence analysis of the entire viral genome from virus recovered from the pigs inoculated with the highest dose of A12-P1 deopt revealed no additional mutations or reversion to the WT virus sequence, and all 489 originally introduced nucleotide changes were maintained. These results indicate that the attenuated phenotype observed in the natural host is directly associated with the changes introduced during the deoptimization process that can determine reduced viral pathogenesis. Likewise, Arzt et al. (31) have proposed that FMDV virulence in another livestock species (cattle) is determined by replication dynamics and the complex interactions between the virus and host innate immune factors at the initial site of infection. However, further studies are required to determine how stable the A12-P1 deopt virus is after repeated passage in primary cell lines and different hosts.

Our results demonstrate that the use of SAVE deoptimization technology is a viable approach to develop attenuated FMDV strains. These attenuated viruses could control a disease outbreak very quickly, since these strains could potentially protect animals as early as 2 days after vaccination, as demonstrated for other attenuated FMDV mutant viruses (13). Furthermore, since attenuation is the result of nucleotide shuffling without changing the amino acid sequence, reversion induced by selective immune pressure is unlikely. Advancement of this technology sounds like an appealing control strategy to be applied in areas where FMD is enzootic to contribute to disease eradication.

ACKNOWLEDGMENTS

This research was supported by USDA CRIS project 1940-32000-057-00D.

We thank J. Robert Coleman and Elizabeth Rieder for helpful discussions, Z. Lu for technical support in DNA sequencing, and the animal care staff at PIADC for their exceptional professional support and assistance with the animal experiments.

FUNDING INFORMATION

U.S Department of Agriculture provided funding to Fayna Diaz-San Segundo, Gisselle N. Medina, Elizabeth Ramirez-Medina, Lauro Velazquez-Salinas, Marla Koster, Marvin J Grubman, and Teresa de los Santos.

REFERENCES

1. **Grubman MJ, Baxt B.** 2004. Foot-and-mouth disease. Clin Microbiol Rev **17:**465–493. http://dx.doi.org/10.1128/CMR.17.2.465-493.2004.
2. **OIE.** 2012. Manual of diagnostic tests and vaccines for terrestrial animals, p 143–173. OIE, Paris, France.
3. **Pluimers FH, Akkerman AM, van der Wal P, Dekker A, Bianchi A.** 2002. Lessons from the foot and mouth disease outbreak in the Netherlands in 2001. Rev Sci Tech **21:**711–721.
4. **Mahy BW.** 2004. Overview of foot-and-mouth disease and its impact as a re-emergent viral infection, p 437–446. *In* Sobrino F, Domingo E (ed), Foot-and-mouth disease: current perspectives. Horizon Bioscience, Portland, OR.
5. **Grubman MJ, Moraes M, Schutta C, Barrera J, Neilan J, Ettyreddy D, Butman B, Brough D, Brake D.** 2010. Adenovirus serotype 5-vectored foot-and-mouth disease subunit vaccines: the first decade. Future Virol **5:**51–64. http://dx.doi.org/10.2217/fvl.09.68.
6. **Glynn I, Glynn J.** 2004. The life and death of smallpox. Cambridge University Press, Cambridge, United Kingdom.
7. **Greenwood B.** 2014. The contribution of vaccination to global health: past, present and future. Philos Trans R Soc B **369:**20130433. http://dx.doi.org/10.1098/rstb.2013.0433.
8. **Roeder P, Mariner J, Kock R.** 2013. Rinderpest: the veterinary perspective on eradication. Phil Trans R Soc B **368:**20120139. http://dx.doi.org/10.1098/rstb.2012.0139.
9. **Moss WJ, Strebel P.** 2011. Biological feasibility of measles eradication. J Infect Dis **204**(Suppl 1)**:**S47–S53. http://dx.doi.org/10.1093/infdis/jir065.
10. **Piccone ME, Rieder E, Mason PW, Grubman MJ.** 1995. The foot-and-mouth disease virus leader proteinase gene is not required for viral replication. J Virol **69:**5376–5382.
11. **Mason PW, Piccone ME, McKenna TS, Chinsangaram J, Grubman MJ.** 1997. Evaluation of a live-attenuated foot-and-mouth disease virus as a vaccine candidate. Virology **227:**96–102. http://dx.doi.org/10.1006/viro.1996.8309.
12. **de los Santos T, Diaz-San Segundo F, Zhu J, Koster M, Dias CC, Grubman MJ.** 2009. A conserved domain in the leader proteinase of foot-and-mouth disease virus is required for proper subcellular localization and function. J Virol **83:**1800–1810. http://dx.doi.org/10.1128/JVI.02112-08.
13. **Diaz-San Segundo F, Weiss M, Pérez-Martín E, Dias CC, Grubman MJ, de los Santos T.** 2012. Inoculation of swine with foot-and-mouth disease SAP-mutant virus induces early protection against disease. J Virol **86:**1316–1327. http://dx.doi.org/10.1128/JVI.05941-11.
14. **Ikemura T.** 1981. Correlation between the abundance of Escherichia coli transfer RNAs and the occurrence of the respective codons in its protein genes: a proposal for a synonymous codon choice that is optimal for the E. coli translational system. J Mol Biol **151:**389–409. http://dx.doi.org/10.1016/0022-2836(81)90003-6.
15. **Jenkins GM, Holmes EC.** 2003. The extent of codon usage bias in human RNA viruses and its evolutionary origin. Virus Res **92:**1–7. http://dx.doi.org/10.1016/S0168-1702(02)00309-X.
16. **Mueller S, Papamichail D, Coleman JR, Skiena S, Wimmer E.** 2006. Reduction of the rate of poliovirus protein synthesis through large-scale codon deoptimization causes attenuation of viral virulence by lowering specific infectivity. J Virol **80:**9687–9696. http://dx.doi.org/10.1128/JVI.00738-06.
17. **Burns CC, Shaw J, Campagnoli R, Jorba J, Vincent A, Quay J, Kew O.** 2006. Modulation of poliovirus replicative fitness in HeLa cells by deoptimization of synonymous codon usage in the capsid region. J Virol **80:**3259–3272. http://dx.doi.org/10.1128/JVI.80.7.3259-3272.2006.
18. **Moura G, Pinheiro M, Arrais J, Gomes AC, Carreto L, Freitas A, Oliveira JL, Santos MAS.** 2007. Large scale comparative codon-pair context analysis unveils general rules that finetune evolution of mRNA primary structure. PLoS One **2:**e847. http://dx.doi.org/10.1371/journal.pone.0000847.
19. **Coleman JR, Papamichail D, Skiena S, Futcher B, Wimmer E, Mueller S.** 2008. Virus attenuation by genome-scale changes in codon pair bias. Science **320:**1784–1787. http://dx.doi.org/10.1126/science.1155761.
20. **Mueller S, Coleman JR, Papamichail D, Ward CB, Nimnual A, Futcher B, Skiena S, Wimmer E.** 2010. Live attenuated influenza virus vaccines by computer aided rational design. Nat Biotechnol **28:**723–726. http://dx.doi.org/10.1038/nbt.1636.
21. **Yang C, Skiena S, Futcher B, Mueller S, Wimmer E.** 2013. Deliberate reduction of hemagglutinin and neuraminidase expression of influenza virus leads to an ultraprotective live vaccine in mice. Proc Natl Acad Sci U S A **110:**9481–9486. http://dx.doi.org/10.1073/pnas.1307473110.
22. **Yu CH, Dang Y, Zhou Z, Wu C, Zhao F, Sachs MS, Liu Y.** 2015. Codon usage influences the local rate of translation elongation to regulate co-translational protein folding. Mol Cell **59:**744–754. http://dx.doi.org/10.1016/j.molcel.2015.07.018.
23. **Atkinson NJ, Witteveldt J, Evans DJ, Simmonds P.** 2014. The Influence of CpG and UpA dinucleotide frequencies on RNA virus replication and characterisation of the innate cellular pathways underlying virus attenuation and enhanced replication. Nucleic Acids Res **42:**4527–4545. http://dx.doi.org/10.1093/nar/gku075.
24. **Le Nouen C, Brock LG, Luongo C, McCarty T, Yang L, Mehedi M, Wimmer E, Mueller S, Collins PL, Buchholz UJ, DiNapoli JM.** 2014. Attenuation of human respiratory syncytial virus by genome-scale codon-pair deoptimization. Proc Natl Acad Sci U S A **111:**13169–13174. http://dx.doi.org/10.1073/pnas.1411290111.
25. **Martrus G, Nevot M, Andres C, Clotet B, Martinez MA.** 2013. Changes in codon-pair bias of human immunodeficiency virus type 1 have profound effects on virus replication in cell culture. Retrovirology **10:**78. http://dx.doi.org/10.1186/1742-4690-10-78.
26. **Shen SH, Stauft CB, Gorbatsevych O, Song Y, Ward CB, Yurovsky A, Mueller S, Futcher B, Wimmer E.** 2015. Large-scale recoding of an arbovirus genome to rebalance its insect versus mammalian preference. Proc Natl Acad Sci **112:**4749–4754. http://dx.doi.org/10.1073/pnas.1502864112.
27. **Wang B, Yang C, Tekes G, Mueller S, Paul A, Whelan SP, Wimmer E.** 2015. Recoding of the vesicular stomatitis virus L gene by computer-aided design provides a live, attenuated vaccine candidate. mBio **6:**e00237-15. http://dx.doi.org/10.1128/mBio.00237-15.
28. **Rieder E, Bunch T, Brown F, Mason PW.** 1993. Genetically engineered foot-and-mouth disease viruses with poly(C) tracts of two nucleotides are virulent in mice. J Virol **67:**5139–5145.
29. **Ni YY, Zhao Z, Opriessnig T, Subramaniam S, Zhou L, Cao D, Cao Q, Yang H, Meng XJ.** 2014. Computer-aided codon-pairs deoptimization of the major envelope GP5 gene attenuates porcine reproductive and respiratory syndrome virus. Virology **450-451:**132–139. http://dx.doi.org/10.1016/j.virol.2013.12.009.
30. **de los Santos T, Diaz-San Segundo F, Grubman MJ.** 2007. Degradation of nuclear factor kappa B during foot-and-mouth disease virus infection. J Virol **81:**12803–12815. http://dx.doi.org/10.1128/JVI.01467-07.
31. **Arzt J, Pacheco JM, Smoliga GR, Tucker MT, Bishop E, Pauszek SJ, Hartwig EJ, de los Santos T, Rodriguez LL.** 2014. Foot-and-mouth disease virus virulence in cattle is co-determined by viral replication dy-

namics and route of infection. Virology **452-453:**12–22. http://dx.doi.org/10.1016/j.virol.2014.01.001.
32. **Alejo DM, Moraes MP, Liao X, Dias CC, Tulman ER, Diaz-San Segundo F, Rood D, Grubman MJ, Silbart LK.** 2013. An adenovirus vectored mucosal adjuvant augments protection of mice immunized intranasally with an adenovirus-vectored foot-and-mouth disease virus subunit vaccine. Vaccine **31:**2302–2309. http://dx.doi.org/10.1016/j.vaccine.2013.02.060.
33. **Mason PW, Grubman MJ, Baxt B.** 2003. Molecular basis of pathogenesis of FMDV.Virus Res **91:**9–32.
34. **Sekiguchi K, Frank AJ, Baxt B.** 1982. Competition for cellular receptor sites among selected aphthoviruses. Arch Virol **74:**53–64. http://dx.doi.org/10.1007/BF01320782.
35. **Devaney MA, Vakharia VN, Lloyd RE, Ehrenfeld E, Grubman MJ.** 1988. Leader protein of foot-and-mouth disease virus is required for cleavage of the p220 component of the cap-binding protein complex. J Virol **62:**4407–4409.
36. **Lobo FP, Mota BE, Pena SD, Azevedo V, Macedo AM, Tauch A, Machado CR, Franco GR.** 2009. Virus-host coevolution: common patterns of nucleotide motif usage in Flaviviridae and their hosts. PLoS One **47:**e6282.
37. **Schneider WM, Chevillotte MD, Rice CM.** 2014. Interferon-stimulated genes: a complex web of host defenses. Annu Rev Immunol **32:**513–545. http://dx.doi.org/10.1146/annurev-immunol-032713-120231.
38. **Salguero FJ, Sanchez-Martin MA, Diaz-San Segundo F, de Avila A, Sevilla N.** 2005. Foot-and-mouth disease virus (FMDV) causes an acute disease that can be lethal for adult laboratory mice. Virology **332:**384–396. http://dx.doi.org/10.1016/j.virol.2004.11.005.
39. **Diaz-San Segundo F, Dias CC, Moraes MP, Weiss M, Perez-Martin E, Owens G, Custer M, Kamrud K, de los Santos T, Grubman MJ.** 2013. Venezuelan equine encephalitis replicon particles can induce rapid protection against foot-and-mouth disease. J Virol **87:**5447–5460. http://dx.doi.org/10.1128/JVI.03462-12.
40. **Pulendran B.** 2009. Learning immunology from the yellow fever vaccine: innate immunity to systems vaccinology. Nat Rev Immunol **9:**741–747. http://dx.doi.org/10.1038/nri2629.
41. **Shearer WT, Fleisher TA, Buckley RH, Ballas Z, Ballow M, Blaese RM, Bonilla FA, Conley ME, Cunningham-Rundles C, Filipovich AH, Fuleihan R, Gelfand EW, Hernandez-Trujillo V, Holland SM, Hong R, Lederman HM, Malech HL, Miles S, Notarangelo LD, Ochs HD, Orange JS, Puck JM, Routes JM, Stiehm ER, Sullivan K, Torgerson T, Winkelstein J, Medical Advisory Committee of the Immune Deficiency Foundation.** 2014. Recommendations for live viral and bacterial vaccines in immunodeficient patients and their close contacts. J Allergy Clin Immunol **133:**961–966. http://dx.doi.org/10.1016/j.jaci.2013.11.043.
42. **Markowitz LE, Preblud SR, Fine PE, Orenstein WA.** 1990. Duration of live measles vaccine-induced immunity. Pediatr Infect Dis J **9:**101–110. http://dx.doi.org/10.1097/00006454-199002000-00008.
43. **Cann AJ, Stanway G, Hughes PJ, Minor PD, Evans DM, Schild GC, Almond JW.** 1984. Reversion to neurovirulence of the live-attenuated Sabin type 3 oral poliovirus vaccine. Nucleic Acids Res **12:**7787–7792. http://dx.doi.org/10.1093/nar/12.20.7787.
44. **Chinsangaram J, Mason PW, Grubman MJ.** 1998. Protection of swine by live and inactivated vaccines prepared from a leader proteinase-deficient serotype A12 foot-and-mouth disease virus. Vaccine **16:**1516–1522. http://dx.doi.org/10.1016/S0264-410X(98)00029-2.
45. **Chinsangaram J, Piccone ME, Grubman MJ.** 1999. Ability of foot-and-mouth disease virus to form plaques in cell culture is associated with suppression of alpha/beta interferon. J Virol **73:**9891–9898.
46. **Wu J, Chen ZJ.** 2014. Innate immune sensing and signaling of cytosolic nucleic acids. Annu Rev Immunol **32:**461–488. http://dx.doi.org/10.1146/annurev-immunol-032713-120156.
47. **Kato H, Takeuchi O, Sato S, Yoneyama M, Yamamoto M, Matsui K, Uematsu S, Jung A, Kawai T, Ishii KJ, Yamaguchi O, Otsu K, Tsujimura K, Koh C-S, Reis e Sousa C, Matsuura Y, Fujita T, Akira S.** 2006. Differential roles of MDA5 and RIG-I helicases in the recognition of RNA viruses. Nature **441:**101–105. http://dx.doi.org/10.1038/nature04734.
48. **Gitlin L, Barchet W, Gilfillan S, Cella M, Beutler B, Flavell RA, Diamond MS, Colonna M.** 2006. Essential role of mda-5 in type I IFN responses to polyriboinosinic:polyribocytidylic acid and encephalomyocarditis picornavirus. Proc Natl Acad Sci U S A **103:**8459–8464. http://dx.doi.org/10.1073/pnas.0603082103.
49. **Hüsser L, Alves MP, Ruggli N, Summerfield A.** 2011. Identification of the role of RIG-I, MDA-5 and TLR3 in sensing RNA viruses in porcine epithelial cells using lentivirus-driven RNA interference. Virus Res **159:**9–16. http://dx.doi.org/10.1016/j.virusres.2011.04.005.
50. **Rima BK, McFerran NV.** 1997. Dinucleotide and stop codon frequencies in single-stranded RNA viruses. J Gen Virol **78:**2859–2870. http://dx.doi.org/10.1099/0022-1317-78-11-2859.
51. **Rothberg PG, Wimmer E.** 1981. Mononucleotide and dinucleotide frequencies, and codon usage in poliovirion RNA. Nucleic Acids Res **23:**6221–6229.
52. **Simmonds P, Tulloch F, Evans DJ, Ryan MD.** 2015. Attenuation of dengue (and other RNA viruses) with codon pair recoding can be explained by increased CpG/UpA dinucleotide frequencies. Proc Natl Acad Sci U S A **112:**E3633–E3634. http://dx.doi.org/10.1073/pnas.1507339112.
53. **Futcher B, Gorbatsevych O, Shen SH, Stauft CB, Song Y, Wang B, Leatherwood J, Gardin J, Yurovsky A, Mueller S, Wimmer E.** 2015. Reply to Simmonds et al.: codon pair and dinucleotide bias have not been functionally distinguished. Proc Natl Acad Sci U S A **112:**E3635–E3636. http://dx.doi.org/10.1073/pnas.1507710112.